Publications

Available Online

J. Sci. Res. **16** (1), 1-16 (2023)

JOURNAL OF SCIENTIFIC RESEARCH

www.banglajol.info/index.php/JSR

Effect of Calcined Eggshell Particleson Some Properties and Microstructure of Al-Si-Mg Alloy

S. C. Eze[1*], D. S. Yawas[2], E. T. Dauda[3]

[1]Mechanical Engineering Department, FOE, Ahmadu Bello University, P.M.B 1094, Samaru. Zaria, Kaduna State, Nigeria

[2]Shell JV Professorial Chair, Mechanical Engineering Department FOE, Ahmadu Bello University, P.M.B 1094, Samaru. Zaria, Kaduna State, Nigeria

[3]Metallurgical and Materials Engineering Department, FOE, Ahmadu Bello University, P.M.B 1094, Samaru. Zaria, Kaduna State, Nigeria

Received 20 October 2022, accepted in final revised form 9 September 2023

Abstract

In this study, different sizes (25, 50, and 75 µm) and volume fractions (1, 2, and 3 wt%) of calcined eggshell particles were utilized to strengthen the Al-Si-Mg alloy. Several experimental runs were conducted to assess the impact of particle size and concentration on both physical properties (density, corrosion, and thermal conductivity) and mechanical properties (hardness, yield strength, impact energy, and modulus of elasticity). The findings revealed significant enhancements in hardness (21 %), yield strength (61 %), modulus of elasticity (43 %), and thermal conductivity (34 %). Conversely, a reduction of 62 % in impact strength and 8 % in density was observed. The corrosion rate displayed an increase from 0 to 16.67 mpy. Analysis using XRD and XRF techniques identified CaO and Al_2O_3 as the primary constituents of the eggshell. Optical micrographs consistently showed cored (segregated) dendritic structures typical of castings cooled under normal conditions in the Al-Si-Mg composite. SEM micrographs, EDS spectra, and area analyses confirmed a uniform distribution of Calcined Eggshell Particles (CEP) within the composite films. Additionally, an optimal calcination condition for the eggshell particles was determined to be 900 °C for 2.5 h, resulting in a CaO yield of 99.62 %.

Keywords: Aluminum profile scraps; Calcination; Composite; Eggshell particles; Microstructure.

doi: http://dx.doi.org/10.3329/jsr.v16i1.62231 J. Sci. Res. **16** (1), 1-16 (2024)

1. Introduction

Composite materials have emerged as crucial components in various industries, notably in automotive manufacturing. These materials offer superior mechanical properties compared to traditional metals and plastics. Among the range of composites available, metal-matrix composites have gained attention for their potential in advancing structural, automotive, aerospace, electronics, wear and thermal management applications. Notably, Hassan *et al*.

[*]*Corresponding author*: samchikeze@gmail.com

[1] reported that metal-matrix composites exhibit exceptional mechanical, physical and thermal properties, including low density, high specific strength, high specific modulus, high thermal conductivity and excellent abrasion and wear resistance.

Aluminum alloys and their composites have garnered significant interest due to the possibility of acquiring the necessary alloy matrix at a reduced cost through secondary manufacturing, utilizing discarded aluminum products like profiles. Extensive research has demonstrated that there is no significant difference in quality between virgin and recycled aluminum alloys. Moreover, incorporating aluminum scraps in the green manufacturing of aluminum alloys/composites for engineering applications offers two advantages: substantial reductions in energy consumption and decreased greenhouse gas emissions associated with primary aluminum production from ore [2-5].

Aluminum profiles, produced by extrusion plants for windows, doors, partitions, and other structures, inevitably generate off-cuts and residues during fabrication. With the construction and housing markets witnessing rapid growth worldwide, it is logical to anticipate an increase in profile consumption and a subsequent rise in off-cuts and residues.

Typically, these residues are either exported for recycling or used in local production for domestic utensils such as pots, plates, and cutlery. However, Alabi et al. [6] highlighted that unregulated recycling activities fail to yield substantial financial benefits and the utilization of aluminum cookware produced from scrap metals has been associated with the leaching of harmful substances, including heavy metals, into cooked food.

From the findings of Dwiwedi *et al.* [7] and Ibrahim *et al.* [8], one essential factor that limits the application of aluminum metal matrix composites is their high cost of production due to the use of expensive synthetic reinforcements such as SiO_2, Al_2O_3, SiC, etc. To overcome this obstacle, researchers have shifted their focus to utilizing low-cost and low-density reinforcements such as eggshells, pumice, bagasse, carbonated coal, and others [1,3,7]. Among these alternatives, eggshells have gained considerable recognition due to their affordability and abundance. Notably, Hayajneh *et al.* [9] reported that eggshell possesses excellent properties, including low density, renewability, eco-friendliness and high thermal stability. As an inedible waste product resulting from egg consumption, eggshells are readily available from hatcheries, residences, and fast food establishments [10]. Global eggshell generation is projected to exceed 8 million tons annually [11,12], indicating an ample and accessible supply of eggshells for particulate reinforcement.

The term ‘calcination,' as used here, refers to heating a substance to a high temperature but below the melting or fusing point, causing loss of moisture, reduction or oxidation and the decomposition of carbonates and other compounds. The calcination of the eggshell is particularly important to remove volatile fractions such as CO_2 and H_2O. The need to achieve a finer particle size and higher CaO content of eggshell powder through calculations was observed by Yang *et al.* [13]. The calcination process is also known to improve the weathering and thermal stability of pigment. This process has been employed by notable scholars [14-18]. However, the literature lacks consensus on the optimum conditions for eggshell calcination.

In this study, the utilization of calcined eggshell particles as low-cost reinforcement in aluminum metal matrix composites is explored.

2. Methodology

2.1. *Processing of eggshells*

Collected eggshells were initially cleaned to remove dirt and then sun-dried for six hours. Subsequently, the dry eggshells were crushed and pulverized using a planetary ball mill machine. To achieve optimal particle size, the pulverized eggshell powder underwent calcination at 900 °C for 2.5 h. The resulting powder was sieved using different mesh sizes (25, 50, and 75 µm) in accordance with the BSI377:1990 standard as described by Biennia *et al*. [19].

2.2. *Processing of aluminum profile scraps*

Al-Si-Mg alloy was obtained from aluminum profile scraps (APS) using the processing technique proposed by Mohammad *et al*. [20]. The temperature during the operation was closely monitored using an optical pyrometer. Finally, the melted aluminum scrap was cast into bars for further processing.

2.3. *Composite blending experiment setup*

The stir-casting process was employed to produce cast ingots of the Al-Si-Mg alloy/eggshell particle composite. A factorial design of 2^k was utilized, with the key input variables being the size of calcined eggshell particles (A) and the concentration of eggshell particles (B). The experimental runs consisted of nine samples with different eggshell particle sizes (25, 50, and 75 µm) and concentrations (1, 2, and 3 wt.%) as shown in Table 1, along with a control sample without the addition of eggshell particles.

Table 1. Out-lay of runs for experiments.

Experimental Run	Al profile scrap ingot (Kg)	CEP size (µm)	CEP concentration Wt %	Composite blend Notation
1	25	25	1	R_1
2	25	50	2	R_2
3	25	75	3	R_3
4	25	25	1	R_4
5	25	50	2	R_5
6	25	75	3	R_6
7	25	25	1	R_7
8	25	50	2	R_8
9	25	75	3	R_9

2.4. *Property tests*

Several properties were investigated in this study, including hardness (H), modulus of elasticity (ME), yield strength (YS), density (D), thermal conductivity (TC), impact energy (IE), and corrosion rate (CR). Standard test specimens were machined from the cast composite blends, and the following tests were conducted:

2.4.1. *Hardness test*

Hardness values were determined using a Rockwell hardness tester (model 38506) in accordance with ASTM E18-19. The test employed a minor load of 10 kg and a major load of 100 kg, with a hardness value of 101.2 HRB on the standard block.

2.4.2. *Tensile tests*

Tensile characteristics, including yield strength (YS) and Young's modulus (ME), were assessed using a testometric tensile testing equipment (model FS300AT) in accordance with the ASTM E8 / E8M standard.

2.4.3. *Thermal conductivity test*

The measurement of thermal conductivity values was performed using Lee's disc method, as described by Singh *et al*. [21], in accordance with the ASTM C 518-15 standard test.

2.4.4. *Impact strength test*

An impact test was conducted using an Avery Denison Notch Bar impact testing machine. A standard circular impact test specimen measuring 75 × 11.4 mm Φ with a notch depth of 2 mm and a notch tip radius of 0.02 mm at an angle of 45° was used according to the ASTM E23-18 standard.

2.4.5. *Density*

Density values were determined by measuring the mass and volume of the specimens using equation 1.

$$\text{Density} = \text{mass/volume (kg/m}^3\text{)} \quad (1)$$

2.4.6. *Corrosion test*

The weight loss and corrosion rate of the specimens were evaluated using the ASTM G31-12 standard laboratory immersion corrosion test technique. The specimens were immersed in a simulated seawater solution prepared with 3.5 g of NaCl per 100 mL of distilled water

for a duration ranging from seven (7) to twenty-one (21) days. The corrosion rate was determined in mils per year (mpy) using equation 2 [22,23]:

$$\text{Corrosion penetration rate (mpy)} = \frac{K\Delta W}{DAT} = \frac{543\Delta W}{DAT} \quad (2)$$

2.5. *Composition and micro-structural examinations*

The elemental composition of the materials (aluminum profile scraps and eggshell particles) was analyzed using a Thermo-Scientific Niton XL 3t XRF analyzer. The morphologies of the control aluminum profile scraps and the composite experimental blends were examined using an NJF-120A metallurgical optical microscope following the ASTM E3-11(2017) standard guide for the preparation of metallographic specimens. Additionally, a Rigaku Mini-Flex300 X-ray diffraction system with PDXL software version 1.8.0.3 was employed to identify the phases present in the sample composite blends, as well as in the raw and calcined eggshell particles.

3. Results and Discussion

3.1. *Chemical composition of eggshell particles*

Table 2. Chemical composition of eggshell particles.

S/N	Element	Composition (wt. %)
1	Al_2O_3	2.000
2	CaO	95.180
3	Fe_2CO_3	0.120
4	CuO	0.006
5	As_2CO_3	0.120
6	SrO	0.559
7	RuO_2	0.340
8	Ag_2O	1.400
9	CeO_2	0.053
10	ErO_2	0.006
11	Yb_2O_3	0.003
12	Ta_2O_6	0.010
13	PbO	0.170

Table 2 shows the chemical composition of eggshell particles. The table shows that CaO and Al_2O_3 were the predominant constituents in raw eggshell particles, which amounts to 95 and 2 wt%, respectively. This observation is consistent with previous studies by Hassan *et al*. [24] and Hussien *et al*. [25]. The test also revealed the presence of hard compounds of Fe_2CO_3, CuO, Ag_2O, Ta_2O_6, and PbO in the composition of eggshell particles.

3.2. *Effect of temperature and dwell time on calcinations of eggshell particles*

The calcination process of eggshell particles was investigated to determine the optimal temperature and dwell time for achieving maximum calcium oxide (CaO) yield. Table 3 presents the different temperature and holding time combinations used in the study. The results showed that the highest CaO yield of 99.62 % was obtained at the optimum conditions of 900 °C and 2.5 h of dwell time. This finding is consistent with previous research by Niju *et al.* [16], Ali *et al.* [15], and Badrul [17], who also obtained optimal results at 900 °C and similar dwell times. These results confirm that calcined eggshell particles can serve as a valuable source of calcium production.

Table 3. Eggshell calcination temperature and dwell time.

Elemental composition	Heating condition				
	900^{o}C for 1 h	900^{o}C for 1.5 h	900^{o}C for 2h	900^{o}C for 2.5 h	900^{o}C for 3 h
S	0.1151	0	0	0	0
K	0.5859	0.1056	0.1724	0	0
Ca	95.3638	99.4823	99.4649	99.6235	99.6234
Ti	0	0.0299	0.0183	0.0341	0.0342
Mn	0.0442	0.0182	0.0152	0.0136	0.0136
Fe	3.3988	0.0504	0.0206	0.0124	0.0124
Co	0	0.0074	0	0.0061	0.0061
Ni	0.0093	0	0	0	0
Zn	0.0025	0.0021	0.0013	0.0016	0.0016
Se	0	0	0	0.0006	0.0006
Sr	0	0.2575	0.2727	0.2856	0.2855
Zr	0.0025	0.0021	0	0	0
Mo	0	0.0006	0.0006	0.0006	0.0006
Pd	0.0026	0.0017	0	0	0
Ag	0.0021	0	0	0	0
Sn	0.005	0	0	0	0
Sb	0.005	0	0	0	0
Te	0.0332	0.0079	0	0	0
Cs	0.0193	0.0066	0.0057	0.0028	0.0028
Ba	0.0795	0.026	0.0235	0.0167	0.0167
Pb	0	0.0018	0.0044	0.0024	0.0025
Th	0	0	0.005	0	0
Total	100	100	100	100	100

Plate 1 provides visual evidence of the influence of calcination temperature and dwell time on the color and pigment texture of the CaO yield. With increasing dwell time, the particles became lighter and brighter. This observation can be attributed to the highly endothermic nature of the reaction involved, which includes the burning of carbon elements.

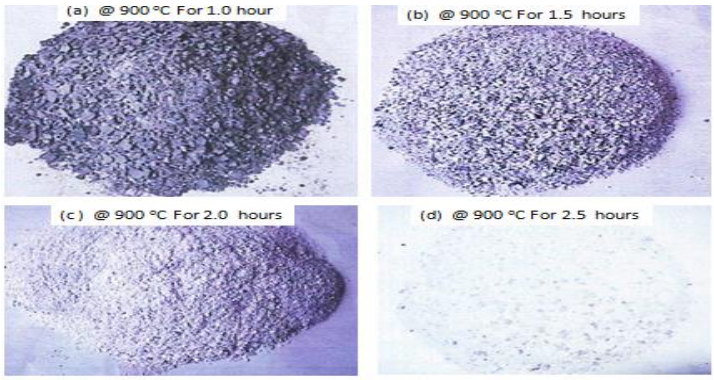

Plate 1. Calcined eggshell particles.

3.3. *XRD examination of raw and calcined eggshell particles*

Figs. 1 and 2 show the results of the XRD obtained using the Cu Kα radiation and d-values spacing of 2θ values for the eggshell particles calcined at the optimum conditions of 900 °C for 2.5 h.

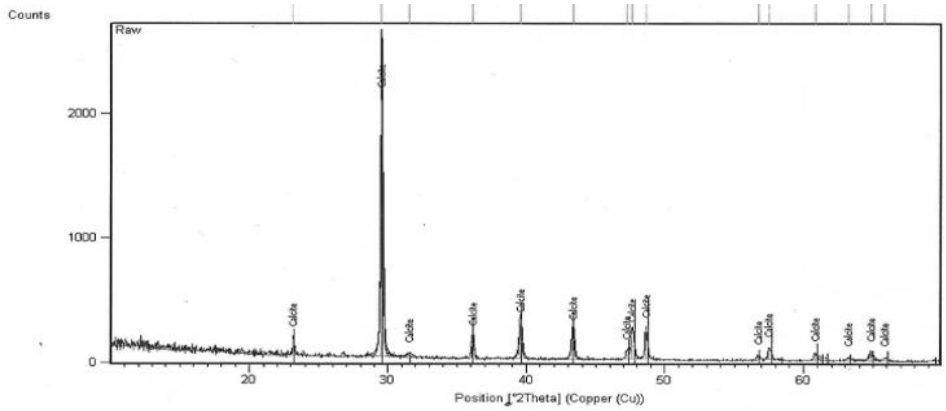

Fig. 1. XRD pattern of raw eggshell particles.

The X-ray diffraction (XRD) analysis results in Figs. 1 and 2 demonstrate the crystalline composition of the raw and calcined eggshell particles at the optimum conditions of 900 °C for 2.5 h. From the XRD spectrum of the raw eggshell particles specimen in Fig. 1, the main peak, which occurred at 2θ = 29.5° revealed a crystalline $Ca_{5.62}Mg_{0.38}C_{6.00}O_{18.00}$ composition with a little trace of magnesium (Mg) presence. In contrast, calcined particles, the presence of the main peak (Fig. 2) appeared at 2θ = 29.5° confirmed the formation of a single phase 'calcite' with a chemical composition of $Ca_6C_6O_{18}$ ($CaCO_3$) and having a hexagonal crystal system. The significant point is that no impurity phase is present in the calcined powders.

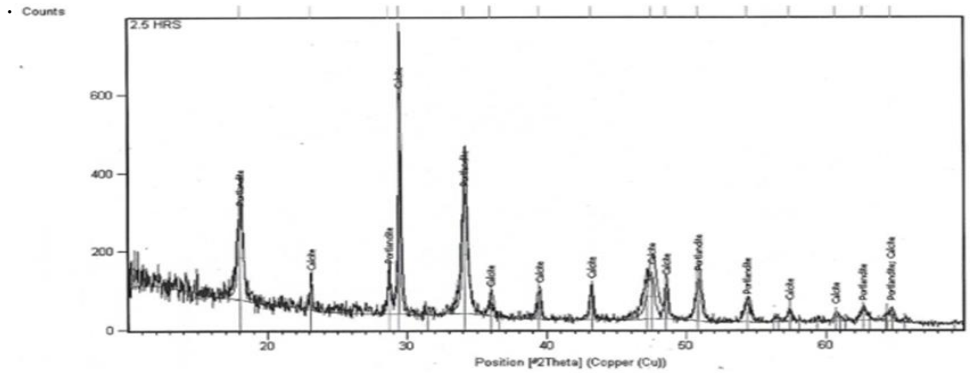

Fig. 2. XRD pattern of calcined eggshell particles.

3.4. *Chemical composition of aluminum profile scraps*

Table 6. XRF result of aluminum profile scraps.

Element	Composition (wt. %)
Mg	7.617
Al	79.210
Si	12.623
S	0.081
Ca	0.060
Ti	0.017
Cr	0.004
Mn	0.019
Fe	0.270
Cu	0.030
Zn	0.046
Sn	0.002
Ba	0.017
Pb	0.004
Total	100.00

Table 6 shows the XRF result of the aluminum profile scrap. The analysis showed that the APS primarily consisted of aluminum (Al), silicon (Si), and magnesium (Mg), which accounted for 99.45 % of the total weight. The aluminum alloys of the 6xxx series contain an excess of Si above that required to form stoichiometric Mg_2Si. The presence of excess Si changes the composition and density of metastable β″ particles. The finding of this study (XRF) supports the designation of aluminum profile scraps used as Al-Mg-Si alloys. Other trace elements, such as zinc (Zn), iron (Fe), and copper (Cu), can help improve the mechanical characteristics of the composite material. Zamani [26] showed that Cu and Mg enhanced the mechanical characteristics of the Al-Si alloy at ambient and increased temperatures, making the alloy heat treatable. The acceptability of high silicon content in these matrix samples is supported by the work of Lee *et al*. [27], who found that the high presence of silicon improves the castability of the composite by improving the fluidity of

the molten composite and allowing it to exhibit excellent dimensional stability, surface hardness, and wear resistant properties.

3.5. *Physio-mechanical properties of composite blends*

Fig. 3(a–g) illustrates the effects of incorporating eggshell particles as reinforcement on the physio-mechanical properties of the composite blends. Compared to the un-reinforced alloy, the reinforced alloy showed significant increases in hardness, yield strength, modulus of elasticity, and thermal conductivity from 30.0 HRB, 42.235 Nmm^2, 7208 Nmm^2, and 83.88 W/mK, respectively, up to maximum values of 36.3 HRB, 68.054 Nmm^2, 38,376 Nmm^2, and 112.23 W/mK, respectively, as shown in Fig. 3 (a-d). However, it was accompanied by a reduction in impact strength and density from raw values of 25 J and 2748 kg/m, respectively, down to 9.5 J and 2529 kg/m^3, respectively, as shown in Fig. 3 (e-f). The increase in hardness, yield strength, and modulus of elasticity can be attributed to the presence of calcined eggshell particles that contain calcite as the major phase and other minor phases that are very hard and brittle. The increase can also be attributed to the difference in the coefficient of thermal expansion between the aluminum alloy and the calcined eggshell particles which increases the dislocation density at the interface. While the decrease in impact can be attributed to the inherent brittleness of the calcined eggshell particles, which amplifies the overall brittleness of the composite material.Furthermore, the decrease in density can be attributed to thelower density of the calcined eggshell particles when compared with the aluminum alloy. This work is on par with the studies conducted by Hassan *et al*. [24], Dwiwedi [8], Feng *et al*. [28], and Ibrahim *et al*. [29].Their findings show that reinforcing alloys with hard particles results in enhanced mechanical properties such as high strength, stiffness, and wear resistance comparedto unreinforced alloys, but at the expense of some ductility.

Fig. 3(g) shows that the corrosion rate increases with increasing eggshell particle content. When comparing the reinforced and non-reinforced aluminum alloys, the non-reinforced aluminum alloy displays a better corrosion resistance rate. The decrease in corrosion resistance can be attributed to the inclusion of eggshell particles, which act as a preferential point for the initiation of corrosion, as reported by Alaneme *et al*. [30].

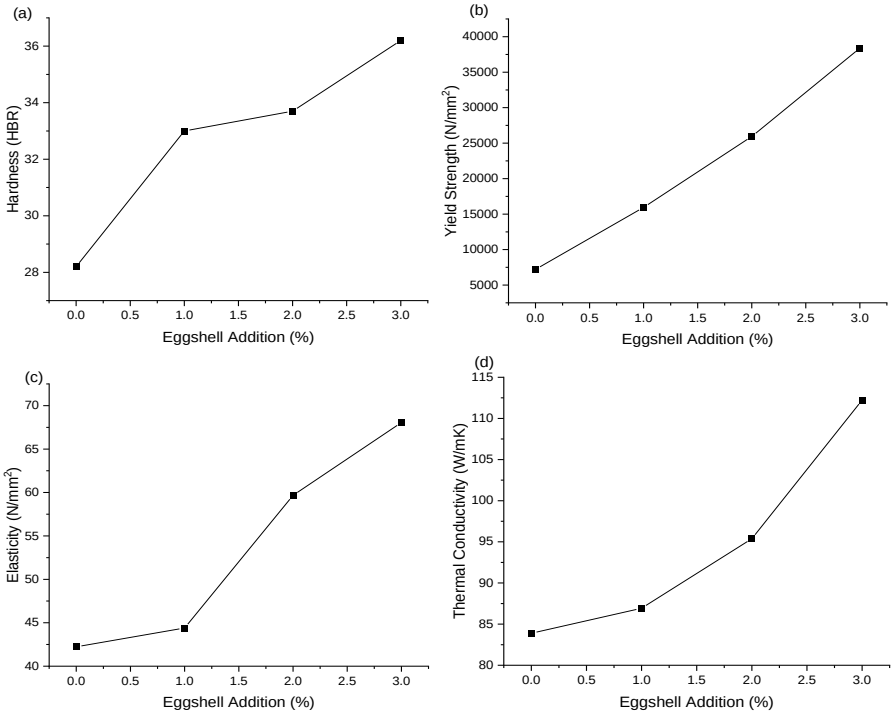

Fig. 3(a-d). Effect of eggshell addition on Hardness, Modulus of elasticity, Yield strength, Thermal conductivity of APS.

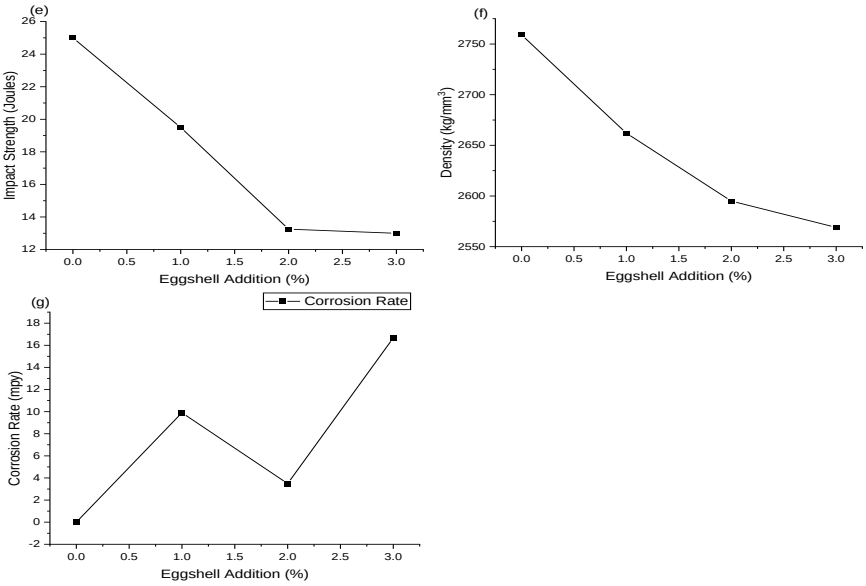

Fig. 3(e-g). Effect of eggshell addition on Impact strength, Density and Corrosion Rate of APS.

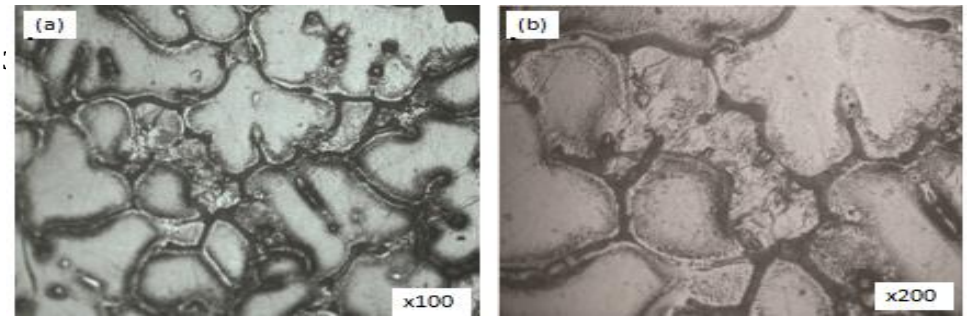

Fig. 4. Optical micrographs of APS control material.

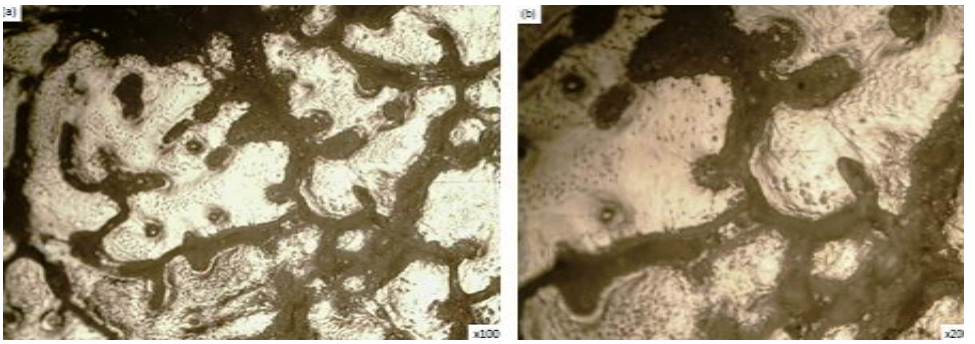

Fig. 5. Optical micrographs of blend with 1 wt.% CEP.

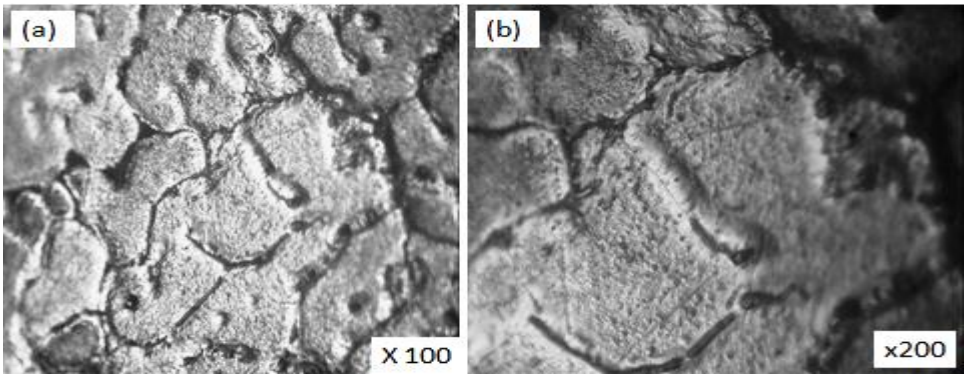

Fig. 6. Optical micrographs of blend with 2 wt.% CEP.

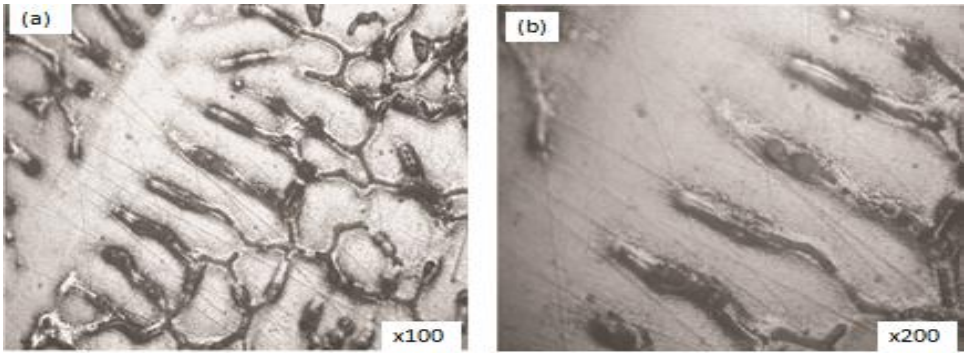

Fig. 7. Optical micrographs of blend with 3 wt.% CEP.

The micrographs in Fig. 4 showed the morphology (structure) of the APS control sample at two magnifications of 100 and 200. In Figs. 5, 6, and 7, the Al-Mg-Si/CEP composite blends contained 1, 2, and 3 wt.% eggshell particle additions, respectively.

In all cases, cored (segregated) dendritic structures are observed, indicative of castings that cooled at moderate rates. Fig. 7 further reveals the presence of intermetallic compound islands (Mg_2Si) that are dark in color around grain boundaries and in the dendritic arms within the aluminum matrix. The addition of eggshell particles alters the morphology of the alloy matrix, and the reaction of eggshell particle constituents with the alloy results in the formation of precipitates during slow cooling. This finding agrees with Lee *et al*. [27], who show that Al-Si alloys solidify by primary precipitation of dendrites. The primary dendrite is seen to be longer (white) with branched secondary arms. The silicon plates are broken down and distributed in the Al-matrix due to the modifying action of calcium present in the eggshell. There are mixtures of intermetallic compounds (Mg_2Si) and particles of eggshells at the grain boundaries. The particles of eggshells (dark particles) were also distributed. It is therefore observed that the inclusion of eggshell particles altered the morphology of the alloy matrix and that precipitates were formed during the slow cooling of the cast due to the reaction of eggshell particle constituents with the alloy.

The results of the scanning electron microscope (SEM) examinations were used to validate the outcome of the optical micrographs.

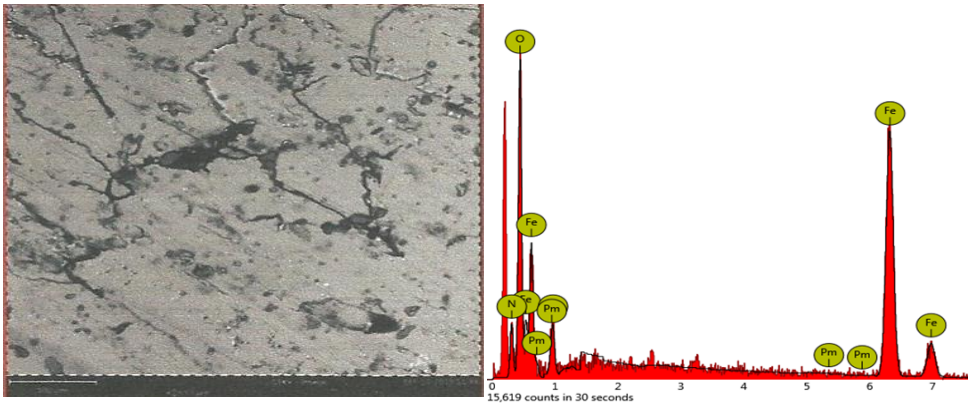

Fig. 8. SEM micrograph and EDS spectrum of Al-Mg-Si/CEPcomposite material.

The analysis of SEM micrographs presented in Fig. 8 also unveiled a dendritic structure characterized by core segregation in the Al-Mg-Si/CEP composite. The corresponding EDS spectrum encompassed a region of micrographs in the CEP 2 wt.% reinforced APS alloy matrix, which show peaks of aluminum (Al), carbon (C), silver (Ag), silicon (Si), iron (Fe), potassium (K), sulfur (S), and the alkaline earth metals calcium (Ca) and magnesium (Mg) as the main constituents of the composite material.

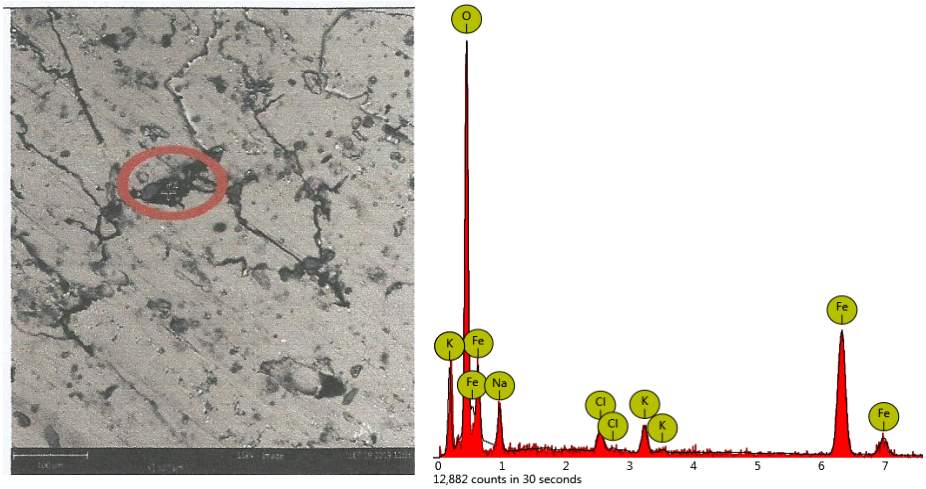

Fig. 9. Spectrum of selected point-1.

\

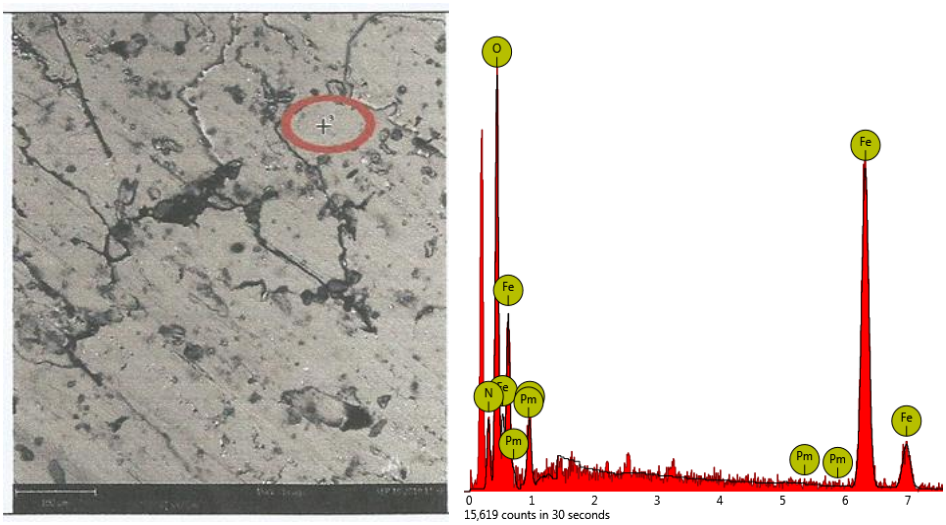

Fig. 10. Spectrum of selected point-2.

The analyses conducted in the vicinity of selected areas of the specimen sample (Figs. 9 and 10) and at varying energy levels revealed the presence of aluminum (Al), carbon (C), silver (Ag), silicon (Si), iron (Fe), potassium (K), sulfur (S), and the following alkaline earth metals: calcium (Ca) and magnesium (Mg). The presence of Ca in these analyses showed that calcined eggshell particles, which are 99.6 % CaO, were present and uniformly distributed in the alloy matrix at the inter-granular and intra-granular regions, as shown in Figs. 9 and 10.

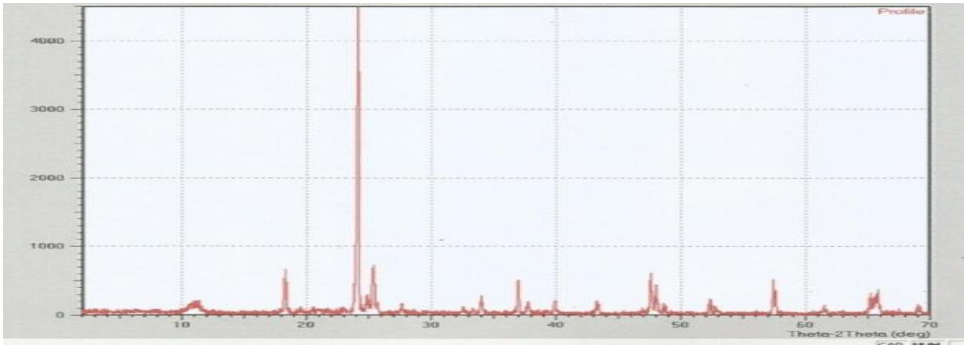

Fig. 11. XRD spectrum of 2 wt.% blend composites.

The presence of these elements was further confirmed by the results of the XRD investigation on the material specimen using d-values spacing of 2θ values, as shown in Fig. 11. It is suggested that the presence of these and other elements from the blend resulted in the formation of various inter-metallic compounds in the microstructure of the composite, such as α-AlO(OH), Fe_3C, TiO_2, $Ca_6Si_6O_{17}(OH)_2$, $CaTiSiO_5$, Al_4C_3,

$NaAlSi_2O_6{\cdot}H_2O$, Al_2O_3, (Mg, Fe, Al)6(Si, Al)4$O_{10}(OH)_8$, $AlNaO_6Si_2$, Mo_2C, $FeCr_2O_4$, and SiC. These inter-metallic phases are associated with the secondary precipitation of Al-Si alloys and add to the composite's characteristics. According to Lee et al. [27], SiC is a very hard phase and thus contributes significantly to an alloy's wear resistance,and when Si combines with other elements,it improvesthe composite's strength and makes it heat-treatable. Calcium, which melts at 842 °C and has a density of 1.55 g/cm^3, contributed substantially to the composite weight reduction and anticipated higher temperature performance. As reported by Kumari *et al*. [31], calcium also acts as a modifier in Al-Si alloys, and also imparts super-plasticity.

4. Conclusion

This study formulated an Al-Mg-Si/CEP composite material by reinforcing processed aluminum profile scraps (APS) alloy with calcined eggshell particles (CEP) using the stir casting technique. It can be concluded:

The optimal conditions for achieving the maximum yield of calcium oxide (CaO) were found to be 900 °C and 2.5 h of dwell time, resulting in a CaO yield of 99.62%. The calcined eggshell particles were found to consist mainly of calcite ($CaCO_3$) with a hexagonal crystal structure, and no impurity phases were detected. Regarding the physio-mechanical properties of the composite blends, the addition of calcined eggshell particles led to significant improvements in hardness, modulus of elasticity, yield strength, and thermal conductivity; in contrast, there were decreases in density, impact strength, and corrosion resistance over the control sample due to the addition of eggshell particles. This showed that calcined eggshell particles could be used as a low-cost, thermally stable reinforcement material to achieve the desired property modification of Al-Si alloys.

References

1. S. B. Hassan and V. S. Aigbodion, J. King Saud Univer. Eng. Sci. **27**, 49 (2015). https://doi.org/10.1016/j.jksues.2013.03.001.
2. N. H. Ononiwu, C. G. Ozoegwu, N. Madushele, and E. T. Akinlabi, Adv. Mater. Proc. Tech. **8**, 411 (2021). https://doi.org/10.1080/2374068X.2021.1959103.
3. J. O. Agunsoye, S. A. Bello, I. S. Talabi, A. A. Yekinni et al., Tribology Industry **37**, 107 (2015).
4. T. K. Ibrahim, D. S.Yawas, B. Dan-asabe, and A. A. Adebisi, Sci. Rept. **13**, 2915 (2023). https://doi.org/10.1038/s41598-023-29839-8
5. S. A. Bello, A. R. Isiaka, and K. R. Nasir, J. King Saud Univer. Eng. Sci. **29**, 269 (2015). https://doi.org/10.1016/j.jksues.2015.10.001
6. O. A. Alabi and Y. M. Adeoluwa, Annals Sci. Tech. **5**, 20 (2020). https://doi.org/10.2478/ast-2020-0003
7. T. K. Ibrahim, D. S. Yawas, B. Dan-asabe, and A. A. Adebisi, Int. J. Adv. Manuf. Technol. **125** 3401 (2023). https://doi.org/10.1007/s00170-023-10923-2
8. S. K. Dwiwedi, K. S. Ashok, S. Koh-ichi, and C. Manoj, Open J. Metal **8**, 1 (2018). https://doi.org/10.4236/ojmetal.2018.81001
9. M. T. Hayajneh, M. A. Almomani, and M. M. Al-Shrida, Sci. Eng. Comp. Mater. **26**, 423 (2019).
10. A. M. King'ori, Int. J. Poultry Sci. **10**, 908 (2011). https://doi.org/10.3923/ijps.2011.908.912

11. F. Alsharari, K. Khan, M. N. Amin, W. Ahmad et al., J. Case Stud. Constr. Mat. **17**, ID e01620 (2022). https://doi.org/10.1016/j.cscm.2022.e01620
12. N. Sathiparan, Constr. Build. Mater. **293**, ID 123456 (2021). https://doi.org/10.1016/j.conbuildmat.2021.123465
13. D. Yang, J. Zhao, W. Ahmad, M. N Amin et al., Constr. Build Mater. **344**, ID 128143 (2022). https://doi.org/10.1016/j.conbuildmat.2022.128143
14. N. Tangboriboon, R. Kunanuruksapong, and A. Sirivat, Mater Sci. Poland **4**, 313 (2012). https://doi.org/10.2478/s13536-012-0055-7
15. A. Ali, H. Jazie, Pramanik, and A. S. K. Sinha - *2nd Intl. Conf. on Power and Energy Systems* (IACSIT, Press, Singapore, 2012) 56.
16. S. Niju, K. M. Meera, S. Begum, and N.Anantharaman, J. Saudi Chem. Soc. **18**, 702 (2014). https://doi.org/10.1016/j.jscs.2014.02.010
17. H. M. Badrul, M. Rahmat, S. Suhandono, F. Syarifah, S. Wiarsih, and F. A. Prakoso - *Proc. of the 3rd Appl. Sci. for Tech. Innovation* (Yogyakarta, Indonesia, 2014) 13.
18. R. A. Rohazriny and N. Ibrahim, in Synthesis and Characterization of Calcium Oxide from Waste Eggshell - *Int. Engr. for Sustainability Conf.* (2014).
19. J. Biennia, M. Walczak, B. Surowska, and J. Sobczaak, J. Optom, Adv. Mat. **5**, 493 (2003).
20. B. N. Mohammad and P. P. Akpan, Leonardo El. J. Pract. Technol. **6**, 71 (2007).
21. R.Singh, G.S. Sandhu, R. Penna, and I. Farina, Materials **10**, 881 (2017). https://doi.org/10.3390/ma10080881
22. M. G. Fontana, Corrosion Engineering, 2nd Edition (McGraw-Hill, New York, 2005) pp. 236.
23. W. D. Callister Jr., Materials Science and Engineering: An Introduction, 7th Edition (John Wiley, 2007) pp. 622-631.
24. S. B. Hassan, V. S. Aigbodion, and S. N. Patrick, Tribology Industry **34**, 217 (2012).
25. H. M. Hussien, Adv. Phys. Theor. Appl. **18** (2013).
26. M. Zamani, PhD Thesis, Jönköping University, Sweden (2017).
27. A. J. Lee, The Minerals, Metals and Mater. Soc. (NASA-M Space Flight Center, Huntsville, 2003).
28. Y. Feng, B. Ashok, S. Naresh, K. Obi-Reddy et al., Int. J. Polym. Anal. Char. **19**, 245 (2014). https://doi.org/10.1080/1023666X.2014.879633
29. K. K. Alaneme and P. A. Olubambia, J. Mater. Res. Technol. **2**, 188 (2013). https://doi.org/10.1016/j.jmrt.2013.02.005
30. T. K. Ibrahim, D. S. Yawas, B. Dan-asabe, and A. A. Adebisi, Funct. Comp. Struct. **5**, ID 015008 (2023). https://doi.org/10.1088/2631-6331/acc0d1
31. S. S. S. Kumari and R. M. Pilla, Int. Mater. Rev. **50**, 216 (2005). https://doi.org/10.1179/174328005X14366